Peptides Hot Paper

How to cite: *Angew. Chem. Int. Ed.* **2021**, *60*, 7333 – 7343
International Edition: doi.org/10.1002/anie.202016208
German Edition: doi.org/10.1002/ange.202016208

Enhanced Live-Cell Delivery of Synthetic Proteins Assisted by Cell-Penetrating Peptides Fused to DABCYL

*Shaswati Mandal[+], Guy Mann[+], Gandhesiri Satish, and Ashraf Brik**

Abstract: *Live-cell delivery of a fully synthetic protein having selectivity towards a particular target is a promising approach with potential applications for basic research and therapeutics. Cell-penetrating peptides (CPPs) allow the cellular delivery of proteins but mostly result in endosomal entrapment, leading to lack of bioavailability. Herein, we report the design and synthesis of a CPP fused to 4-((4-(dimethylamino)phenyl)azo)benzoic acid (DABCYL) to enhance cellular uptake of fluorescently labelled synthetic protein analogues in low micromolar concentration. The attachment of cyclic deca-arginine (cR10) modified with a single lysine linked to DABCYL to synthetic ubiquitin (Ub) and small ubiquitin-like modifier-2 (SUMO-2) scaffolds resulted in a threefold higher uptake efficacy in live cells compared to the unmodified cR10. We could also achieve cR10DABCYL-assisted delivery of Ub and a Ub variant (Ubv) based activity-based probes for functional studies of deubiquitinases in live cells.*

Introduction

Cell-permeable synthetic proteins possess the power to advance our knowledge of intracellular protein-protein interactions, protein localization and functions. Intracellular delivery of biologically relevant proteins, particularly those having crucial cellular functions to disease state could find useful applications for basic research and as therapeutics.[1] However, due to their physical properties, proteins cannot often cross the plasma membrane without utilizing delivery methods.[2] In this regard, cell-penetrating peptides (CPPs) have gained numerous research interest because of their potential to deliver cargo into live cells by covalent or affinity interaction with the cargo.[3] Although the early CPPs were natural protein derived peptides (e.g. TAT, penetratin), synthetic CPPs with complex modifications are reported to outperform the conventional CPPs.[4,5] Interestingly, cyclization plays an important role in increasing the efficiency of the CPPs to penetrate the cell membrane due to structural rigidity[6] and high proteolytic stability.[7] Additional improvement of CPP properties can be achieved by increasing the number of the positive charge of the CPP,[7,8] the addition of inverted chiral residues (i.e. D-amino acids),[9] and in some cases the addition of hydrophobic side chains at specific sites (e.g. palmitoylation).[10]

CPP-protein conjugates mostly enter into cells via endocytosis and reach the cytosol only if successful endosomal escape takes place.[2] The process of endosomal escape is unpredictable and its efficiency varies for different CPP-cargo conjugates, resulting in one of the major drawbacks in CPP mediated protein delivery.[5] Endosomally trapped protein cargos undergo lysosomal degradation by lysosomal proteases,[11] which eventually prevents the cellular uptake analysis of protein. Achieving a uniform cytosolic distribution of proteins in low concentration is very challenging in terms of cost-efficiency.[12] Live cell delivery of proteins with high efficacy is necessary for the proficient analysis of the protein function. Moreover, there are only a few examples for the delivery of fully synthetic[13–15] or semi-synthetic[16,17] proteins, having different labels and backbone modifications into live cells.

To overcome the current limitations, we attempted to develop a new class of CPP, which will be added to the chemical biology toolbox for efficient intracellular delivery of synthetic proteins. We chose to work with fluorescently labelled synthetic mono-ubiquitin (Ub) scaffold as our primary protein of interest since it plays important roles in maintaining various cellular functions. An important part of the Ub machinery is the deubiquitinating enzymes (DUBs), which regulates Ub homeostasis. We and others have reported several synthetic strategies based on various ligation approaches to generate different Ub or polyUb chains with functional labels and also poly-ubiquitinated proteins with precisely branched native and non-native bonds.[18–20] These strategies offer unprecedented control over the Ub scaffold or chain, the linkage-types and lengths, which demonstrated great value in the areas of Ub research.[21] These strategies have also been adopted to Ub-like (Ubl) modifiers, such as small Ub-like modifier (SUMO).[22–25]

Herein, we report on the design and synthesis of a new CPP, which highly improves the cytosolic delivery of CPP-protein (Ub and SUMO-2) conjugates in low micromolar concentration. The uptake efficiency of our synthetic proteins was confirmed by qualitative live-cell confocal laser scanning microscopy (CLSM) and statistically analyzed by imaging flow cytometry. We have successfully demonstrated the live-cell delivery of Ub based activity-based probe (ABP), carrying a C-terminal propargylamine (PA) warhead, which can covalently trap different intracellular enzymes of the

[*] S. Mandal,[+] G. Mann,[+] Dr. G. Satish, Prof. A. Brik
Schulich Faculty of Chemistry, Technion-Israel Institute of Technology
3200008 Haifa (Israel)
E-mail: abrik@technion.ac.il

[+] These authors contributed equally to this work.

Supporting information and the ORCID identification number(s) for the author(s) of this article can be found under: https://doi.org/10.1002/anie.202016208.

ubiquitination system.[26,27] Alongside, we successfully delivered an Ub variant (Ubv), bearing a PA warhead for labelling intracellular Ub specific proteases 7 (USP7).

Results and Discussion

Design and Synthesis of New CPP Linked to Fluorescently Labelled Peptides

The rational design for this study includes fluorescently labelled synthetic Ub scaffold fused with a disulfide-linked cleavable CPP moiety at the N-terminus. We choose the cleavable cyclic deca-arginine peptide (**cR10**) as a model CPP as it shows three times more uptake efficiency for the GFP binding protein antibody compared to cTAT peptide and also it is recently reported to have efficient cellular uptake of mCherry.[12,28] Although, our previous findings demonstrated delivery of Ub analogues modified with the reported cyclic deca-arginine (**cR10**) through a stable linkage,[15] the N-terminal disulfide-linked **cR10** (cleavable) seemed to be inefficient in endosomal escape (results not shown). As of today, only a few studies have been reported on the live-cell delivery of synthetic CPP-Ub conjugates. Yet, in all these studies substantial endosomal entrapment was observed.[16] Withstanding in this situation, where efficient live-cell delivery of synthetic Ub/Ub like conjugates is currently a challenge with no universally accepted regimen, we aimed to design a new CPP to promote efficient cellular uptake and benefit from this developed synthetic tools in the Ub/ Ubl research fields.

We chose to modify **cR10** with 4-(dimethylaminoazo) benzene-4-carboxylic acid (DABCYL) because of its structural simplicity, availability along with hydrophobicity, which could assist cell permeability. First, we aimed to compare the efficiency of the CPPs in a small peptide system containing a fluorescently labelled short peptide (**P1** labelled with fluorescein isothiocyanate, FITC), which was synthesized using SPPS, (Figure 1a). The CPP units (**cR10** and **cR10DABCYL**) were synthesized and activated using modifications of the reported procedure (Figure 1b, Figure S2).[28] Peptide **P1** was conjugated to the activated CPPs via a cleavable disulfide linkage to afford peptides **1** and **2** respectively, as shown by HPLC-MS analysis (Figure 1c,d).

DABCYL-Modified CPP Promotes the Efficient Cellular Uptake of Peptides

Endocytic cellular uptake of CPP-linked peptides (or proteins) mostly lead to punctuate signals indicative of the cargo entrapment inside the endosomal compartments. Efficient endosomal escape of the cargo is highly necessary for bioavailability and bioactivity. To verify the improvement in live-cell delivery of the peptide linked to **cR10DABCYL** (**cR10D**), we co-incubated U2OS cells with 6 μM of **1** and **2** dissolved in phosphate buffer saline (PBS). After 15 min of co-incubation, we performed heparin sulfate washing to remove membrane-bound peptides. The delivery was followed by the FITC fluorescence signal and analyzed by CLSM (Figure 2).

By observing the live-cell images with the two different CPPs, we were pleased to observe enhanced delivery for peptide **2**. Peptide **1** was mainly stuck in the membrane and endolysosomal compartments (as green punctuates), whereas **2** was uniformly distributed into the cytosol (Figure 2a,c).

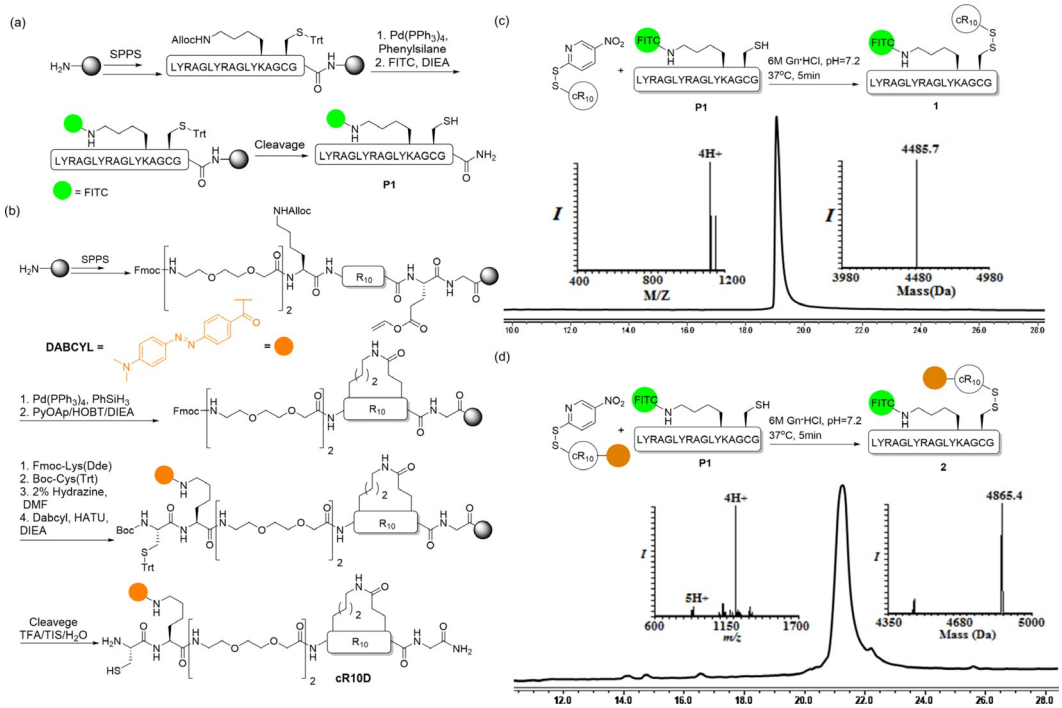

Figure 1. Chemical synthesis of model peptides **1** and **2**. a) Synthetic scheme for **P1**. b) Synthetic scheme for **cR10D**. c) Conjugation of activated **cR10** to **P1** and HPLC-MS analysis of purified **1**. d) Conjugation of activated **cR10D** to **P1** and HPLC-MS analysis of purified **2**.

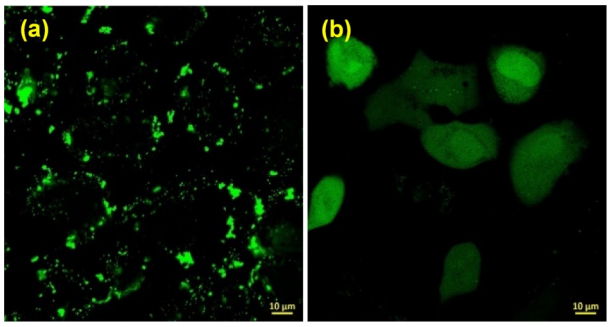

Figure 2. Delivery of model peptides **1** and **2** to live U2OS cells. a) FITC signal from **1** (green). b) FITC signal from **2** (green) (scale bars 10 μm).

From these experiments, we concluded that **cR10D** exhibited efficient cell delivery when compared to the unmodified **cR10**, where Lys-linked DABCYL appears to assist in the cellular uptake or endosomal egress of the model peptide (**P1**).

With these results in hand, we turned to implement the DABCYL effect in a biologically relevant protein, such as Ub. Ubiquitination, the attachment of a Ub or polyUb chain to a protein target regulates many cellular processes such as protein trafficking and degradation, signal transduction, DNA repair and cell division.[19,29] Ubiquitination is a reversible process, in which DUBs removes Ub or the polyUb chain from the substrate protein.[30] DUBs are considered key players in Ub signaling and function at various stages of the Ub life cycle, starting from the generation of mature Ub from inactive fusion proteins to the control of the function and destiny of ubiquitinated proteins by removing or editing the Ub chain.[31] A large section of the accumulated knowledge about DUBs has been obtained using various methods like small molecule inhibitors,[32,33] and activity-based probes,[21] which supported DUB's important roles in various diseases.

Synthesis of CPP-Ub Conjugates for Cellular Uptake Experiment

Development of synthetic strategies to Ub conjugates has contributed to the experimental approaches to study the Ub system. Despite these impressive synthetic achievements, homogenously ubiquitinated proteins have been mainly used for in vitro experiments, a simplified representation of the cellular environment lacking distinct cellular regulatory elements and biological context.[16] In light of this limitation, the area of Ub research would tremendously benefit from methods that allow the delivery of synthetic Ub probes into live cells.

In this study, we synthesized Ub analogues with a PEG linker bearing a Cys residue in its N-terminal to mediate disulfide linkage with the CPP, while the N-terminus is labelled to a fluorophore 5-carboxytetramethylrhodamine (TAMRA). The synthesis was carried out using Fmoc-SPPS on 2-chlorotrityl chloride resin (2-CTC) and the final construct TAMRA-Cys-Ub-COOH (**3**) was purified in 19% yield (Figure S6). To obtain the final Ub conjugates with the two different CPPs, both of the activated (DTNP switched) **cR10** and **cR10D** were reacted with **3** in 6 M Gn·HCl at pH ≈7.2 for 5 min to generate Ub analogues **4** and **5** in 56% and 60% isolated yield, respectively, (Figure 3b,c).

A threefold increase in the efficiency of live cell delivery of synthetic Ub linked to DABCYL-**cR10** in comparison to unmodified **cR10**: After synthesizing the Ub analogues **4** and **5**, we examined the efficiency of the CPPs in live-cell delivery. We treated U2OS cells with 2 μM of **4** and **5**, followed by 1 h incubation and staining with Hoechst (nuclear stain).

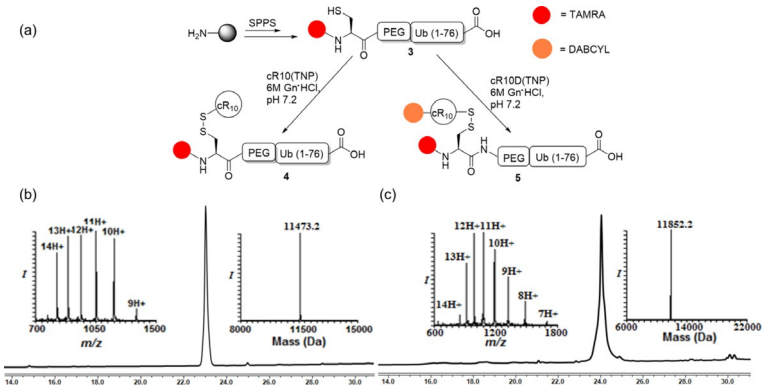

Figure 3. Synthesis of Ub-conjugates: a) Synthetic scheme of **4** and **5** starting from **3**. b) HPLC-MS analysis of purified conjugate **4** (observed mass = 11 473.2 ± 0.2 Da, calcd mass = 11 473 Da). c) HPLC-MS analysis of purified conjugate **5** (observed mass = 11 852.2 ± 0.2 Da, calcd mass = 11 852 Da).

The CLSM images confirmed that analogue **5** is uniformly delivered in the cytosol and localized in the nucleus and nucleoli, with significantly fewer signals in the lysosomes or endosomes as compared to analogue **4** (Figure 4a,e). The enhanced live-cell delivery with **cR10D** was verified by the *Z*-stack images as well (Figure S9). Additionally, the cellular uptake of **4** and **5** at 4 μM was studied in the presence of DMEM cell culture medium containing serum (FBS). As Ub analogues freely diffuse into the nucleus after reaching cytosol due to their small molecular weight (≈8 kDa)[34,35] and as the nucleus is deprived of any endosomes or lysosomes, we used the nuclear masking strategy following nuclear TAMRA intensity to assess the efficiency of delivery. The quantification of the total nuclear TAMRA intensity inside U2OS cells (over 150 cells), using FiJi software depicted a threefold increase in fluorescence intensity for **cR10D** compared to **cR10** (Figure 4i, Figure S8, S9). After confirming that DABCYL assisted efficient delivery of synthetic Ub probes, we wanted to verify that the increased fluorescence correlates to the amount of TAMRA-Ub in the delivered cells. For this, we analyzed the U2OS cell lysates upon cell delivery by SDS-PAGE. Prior to lysis, cells were washed by trypsin-EDTA solution and vigorous cold PBS washes were performed to remove any non-internalized CPP-cargo construct.[36,37] Fluorescent SDS-PAGE following TAMRA emis-

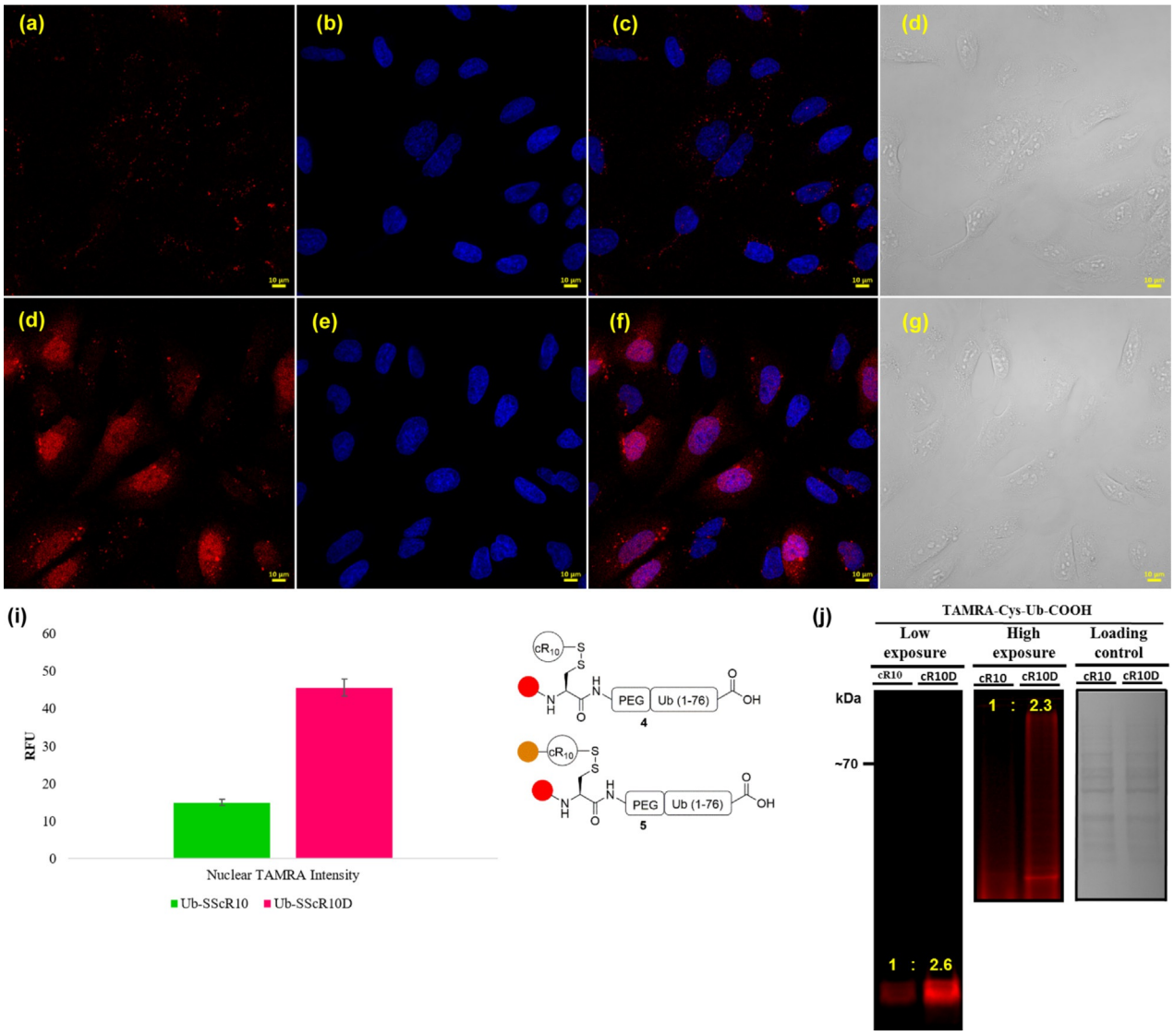

Figure 4. Representative images of delivery of Ub analogues **4** (a–d) and **5** (d–g) to live U2OS cells. a,d) **4** and **5** (TAMRA, red). b,e) Hoechst (blue). c,f) TAMRA and Hoechst channels combined. d,g) Bright field channel. (Scale bars 10 μm). The experiment was repeated twice. i) Quantification of nuclear TAMRA intensity relative to the untreated cells from Figure 4a & e. Results are the average of two independent experiments (over 150 cells per experiment). Error bars are the standard deviation of the averages. j) Fluorescent gel assay in U2OS cells after cell delivery.

sion demonstrated that the delivery of the conjugated and free probe was more for **cR10D** than **cR10** (Figure 4j).

Linear R10DABCYL Delivers Ub Scaffold with Similar Efficiency as Cyclic cR10DABCYL

Next, we wanted to examine the effect of DABCYL on the linear CPP and compare its efficiency in cell delivery. It has been recently discovered that cyclization of CPPs enhances their cellular entry efficiencies.[6,8] Therefore, we designed the linear deca-arginine peptide modified with Lys linked DABCYL (**R10D**). In addition, we wanted to examine if the observed increase in protein delivery is due to the loss of the lysosomal signals, as a result of the quenching effect of DABCYL on TAMRA fluorescence, or because of increase in the total amount of proteins delivered in live cells. Therefore, we introduced Black Hole Quencher 2 (BHQ2), which is known to quench TAMRA fluorescence efficiently and modify the CPP, similarly to the **cR10D.** The linear R10 modified with DABCYL (**R10D**) and **cR10** modified with BHQ2 (**cR10BHQ2**) were incorporated at the Lys side chain, to maintain the structural similarity with **cR10D**. Cleavage from the solid support followed by purification gave **R10D** and **cR10-BHQ2** in isolated yields of ≈13% and ≈10%, respectively, (Figure S10, S11). To compare the efficiency of the four addressed CPPs, we synthesized fluorescently labelled Ub with amide functionality in the C-terminus. The synthesis was carried out in a similar manner using Fmoc-SPPS on Rink amide resin to afford **6** in 10% isolated yield (Figure S12). Upon activation of the Cys group for each CPP, these were subsequently reacted with TAMRA-Cys-Ub-

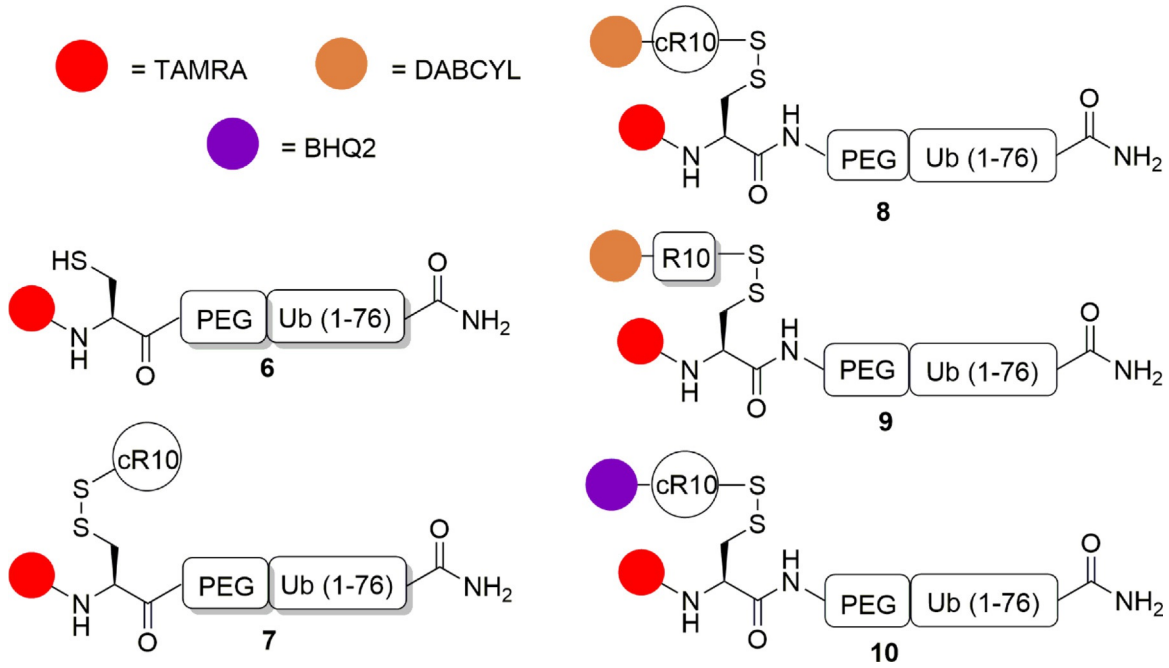

Figure 5. TAMRA-Cys-Ub-$CONH_2$ construct (**6**) and the four fluorescently labelled Ub-CPP conjugates (**7**–**10**) for live-cell delivery.

$CONH_2$ through disulfide bond exchange reaction to give **7**–**10**, Figure 5 (Figure S13).

The CLSM images (Figure 6) confirmed an increase in TAMRA (red) fluorescence when HeLa cells were treated with **cR10D**-containing Ub analogue (**8**) compared to those treated with TAMRA-Cys(**cR10**)-Ub (**7**), Figure 6a,f. A similar fluorescence increase was observed for the linear **R10D** (**9**) suggesting that attachment of DABCYL to linear R10 enhanced the cellular uptake of fluorescently labelled Ub constructs with significantly less endosomal or lysosomal entrapment (Figure 6k). Surprisingly, BHQ2 modification did not increase the efficiency of delivery as confirmed by the TAMRA intensity in the respective CLSM images (Figure 6p). The efficient intracellular delivery of both the cyclic and linear DABCYL CPPs suggests that DABCYL could compensate to large extent on the absence of structural rigidity and that cyclization is not mandatory for enhanced cellular uptake efficiency of fluorescently labelled Ub constructs. This indeed indicated that the DABCYL effect on the cellular uptake efficiency for synthetic Ub probes could be not only due to its hydrophobic contribution but also due to unique structural features that are yet to be determined.

After confirming the delivery of **7**–**10**, the TAMRA intensity measured by CLSM was analyzed by FiJi software under CT-DR mask and nuclear mask (Figure 7a, S14). Our results suggest that the cells treated with **8** and **9** containing **cR10D** and **R10D** respectively, appear to have a similar abundance of fluorescence intensity. Notably, the cell mask did not represent the actual cytosolic TAMRA intensity measurements for different Ub probes. This is probably due to the high fluorescence from the endosomally trapped proteins for **7** or **10**, where the cytosolic availability of protein was not improved.

To strengthen our results, along with the confocal microscopy study we used a robust flow imaging cytometry method, which enabled the detection of delivery efficiency at a single-cell level providing a large data set. The experiment was done by co-incubating U2OS cells with 2 μM of analogues **7** and **8** dissolved in PBS. The cell delivery was followed by LT-G staining, harvesting the cells by trypsin and lastly, adding Hoechst stain. Again, nuclear localization of the fluorescently labelled Ub analogues (**7** and **8**) was used as a metric to determine efficient cell delivery applied to the gained data set as a series of gates.[38] Interpreting the statistical image analysis data, it can be comprehended that the **cR10D** is three times better in the delivery of the Ub analogue to U2OS cells than **cR10** (Figure 7b).

CPPs are known to strongly bind to the cell membranes and were reported to compromise the membrane integrity at high concentrations.[39] Although we used concentration that is safe and below the reported toxic range of **cR10**,[28] we verified that the addition of DABCYL does not compromise membrane integrity by using SYTOX blue™ as previously reported.[15] In our delivery conditions we could not detect any cells with compromised plasma membrane as evident by a complete uniform population of SYTOX blue negative cells in all the **cR10D** concentrations that were measured (Figure S17).

Live-cell Delivery of Ub- and Ubv-Based ABP

Among ≈100 DUBs in a human genome, most of them are cysteine proteases.[18,40] Previous reports established that C-terminally attached alkynes to a substrate protein can react with the active-site Cys of target proteases, which will be denaturation resistant.[26] C-terminally propargylated Ub was

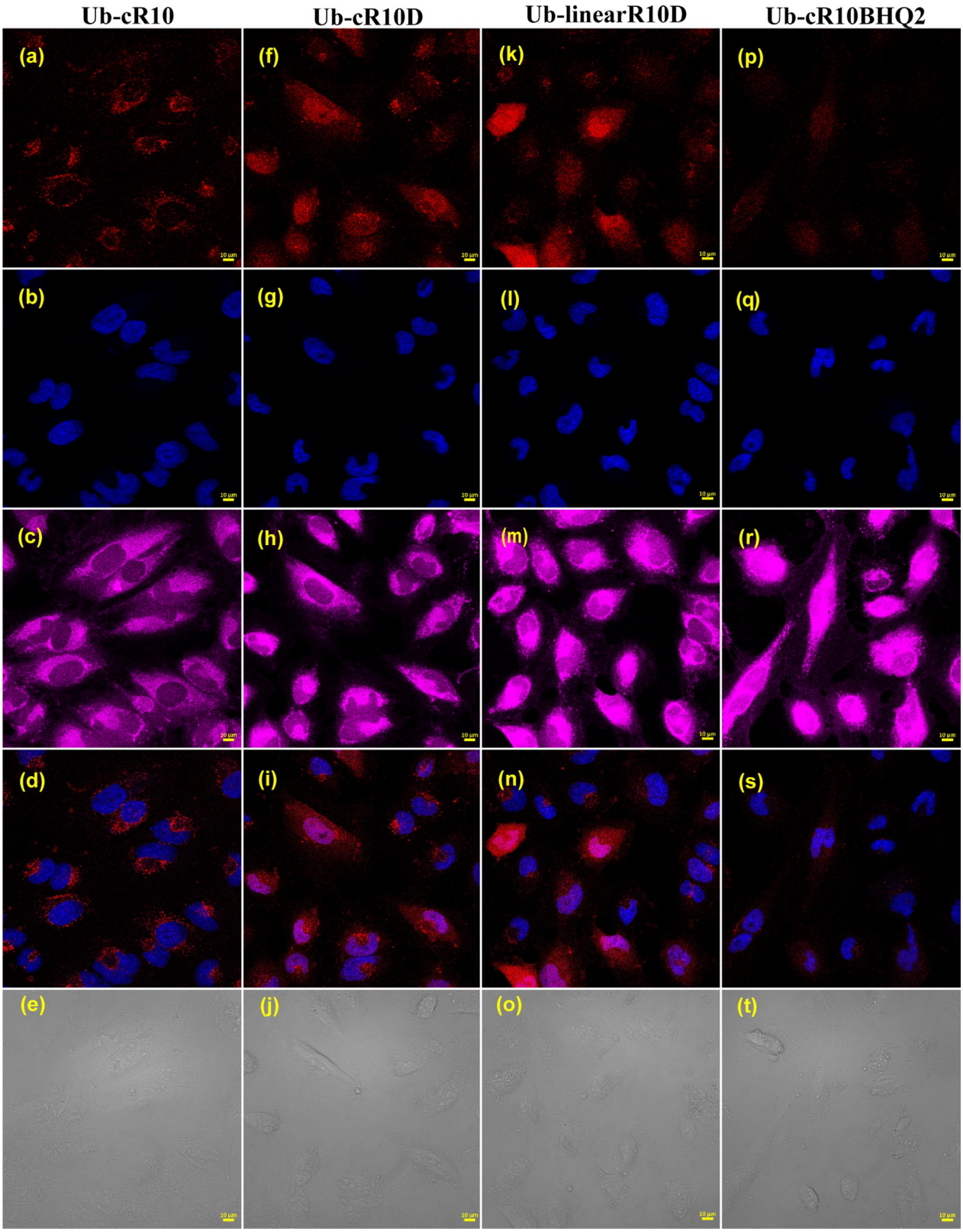

Figure 6. Representative images of delivery of **7**, **8**, **9**, **10** to live HeLa cells. a,f,k,p) TAMRA signal (red) from **7**, **8**, **9**, and **10**, respectively. b,g,l,q) Hoechst (blue) from **7**, **8**, **9**, and **10**, respectively. c,h,m,r) CT-DR (pink) from **7**, **8**, **9**, and **10**, respectively. d) **7** (TAMRA) and Hoechst channel from (a) and (b) combined. i) **8** (TAMRA) and Hoechst channel from (f) and (g) combined. n) **9** (TAMRA) and Hoechst channel from (k) and (l) combined. s) **10** (TAMRA) and Hoechst channel from (p) and (q) combined. e,j,o,t) Bright field images from **7**, **8**, **9**, and **10**, respectively. (Scale bars 10 μm). The experiment was repeated three times.

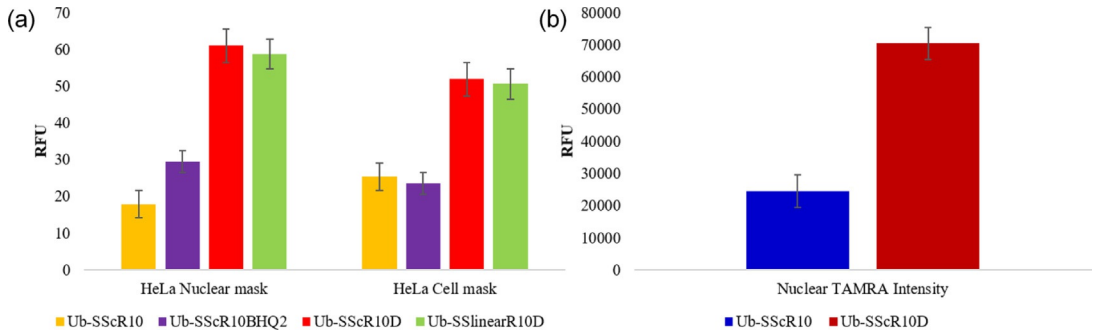

Figure 7. Quantification of cellular and nuclear TAMRA intensity in a) HeLa cells after treatment with **7**–**10**, relative to untreated cells (based on the average of 450 cells from three repetitions). b) Quantification of nuclear TAMRA intensity after treatment of U2OS cells with **7** and **8**, as determined by flow imaging cytometry. Unpaired t-test, $p < 0.0001$. Results are the average of two independent sets of experiments. Error bars are the standard deviation of averages.

also reported as a potential candidate as an activity-based probe (ABP) for labelling various DUB.[27] With our efficient delivery vehicle, we then attempted the cell delivery of Ub based ABP. Hence, we designed an Ub probe having a solvent-exposed S20C mutation for incorporating the **cR10D** unit. Also, G76 of Ub was replaced with propargylamine (PA) warhead and a fluorescent label (TAMRA) at N-terminus to monitor the live-cell delivery followed by fluorescent gel analysis.

Among the various members of DUBs, Ub specific protease 7 (USP7 or HAUSP) is a human DUB known for regulating the cellular level of tumour suppressor p53.[41] Due to the deviant expression of USP7 in many human cancers and other diseases, this particular DUB became a potent target for cancer therapy.[42] We chose to target USP7 by utilizing Ubv based ABP. Binding of Ub with proteins generally occurs via Ub binding domain (UBD) with low affinity and in an unspecific manner.[43] The Ub affinity can be tuned to be enhanced towards a particular enzyme by mutating different positions of the Ub sequence to generate Ub variants (Ubv).[43] One of these variants is the M6 containing PA warhead in the C-terminus, which was found to be very selective for USP7 in HAP1 cell lysate.[44] This M6 was reported to have mutations at several positions in comparison to Ub (T7D, L8Y, I13R, E34L, Q40N, D58K-biotin, L69A, and L71A). The presence of a bulky group at K_{58} position (lysine-biotin) was introduced to hinder the interaction of M6 with USP5,[44] which substantially contributed to its selectivity towards USP7. To enable live-cell delivery of the Ubv based USP7 ABP i.e., M6, we also mutated the solvent-exposed Ser20 residue into Cys to allow incorporation of **cR10D** through disulfide linkage.

Both Ub and M6 were synthesized on SPPS using reported linker o-amino(methyl)aniline (MeDbz) followed by on resin ammonolysis to get TAMRA-Ub(S20C)-PA and TAMRA M6(S20C)- PA in 10% and 7% isolated yields, respectively. Next, both of the analogues were conjugated to the activated **cR10D** peptide affording construct **11** and **12** (Figure 8a,b).

Next, we proceeded to perform live-cell delivery of both Ub and Ubv based DUB ABP (**12**). Both analogues **11** and **12** were successfully delivered in U2OS cells by co-incubating 4 μM of each conjugate dissolved in PBS for 1 h. In the case of Ub-PA analogue (**11**), the delivery was significantly good in 2 μM concentration, (Figure S23). However, with the M6 construct (**12**) we had to increase the concentration to 4 μM to get similar efficiency of delivery to **11** probably due to the different mutations and modifications performed compared to the other Ub analogues. CLSM images verified that the Ub based ABP can also be efficiently delivered into the U2OS cells by changing the CPP position from N-terminal to a solvent-exposed area (Figure 9a). The M6 delivery (Figure 9e) possibly could be improved by removing the biotin tag.

To confirm the M6 selectivity towards USP7 following delivery in live cells, we carried out SDS-PAGE and western blot (WB) analysis with U2OS cell lysate (Figure S24). The selectivity of M6 towards USP7 was at first confirmed by the reactions of the probes with cell lysates as a positive control. Analysis of lysates from U2OS cells upon delivery of **11** and **12** by gel-based fluorescence and WB against USP7 demonstrated that USP7 was selectively labelled by M6 in live cells, (Figure S24). While comparing the lysate and live-cell results, we observed that treating cell lysates with the Ub probe resulted in a similar number of fluorescent bands (Figure S24a,b) when compared to live U2OS cells treated with the Ub probe, (the difference was more prominent in the high molecular weight region). Our lysis condition was designed to prevent the post lysis reactions between the residual undelivered probes and the enzymes released during lysis. Therefore, these results support the applicability of our approach in live-cell delivery of synthetic Ub probes and labelling of different cellular components. Also, the M6-ABP demonstrated identical USP7 labelling both in lysate and live cells. These results suggest that the activity profile of USP7 is unaltered upon cell lysis and could be studied using cell lysates for development of new USP7 inhibitors.

Synthesis of CPP-SUMO-2 Conjugates for Cellular Uptake Experiments

The post-translational modification of proteins with SUMO, known as SUMOylation regulates a plethora of cellular processes. Chemical and semi-synthesis of different SUMO analogues or SUMOylated proteins intrigued us to

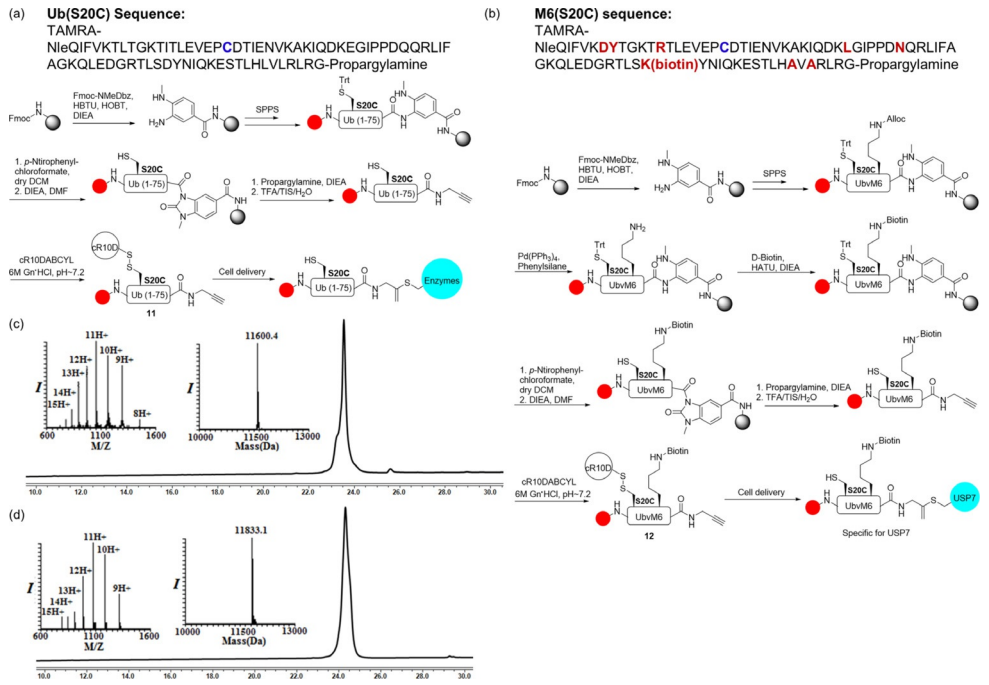

Figure 8. Synthesis of cell-permeable DUB ABP. a) Ub sequence with S20C mutation and synthetic scheme for Ub-based DUB ABP (**11**) for live-cell delivery. b) Ubv M6 sequence with S20C mutation and synthetic scheme for Ubv-based DUB ABP (**12**) for live-cell delivery. c) HPLC-MS analysis of purified conjugate **11** (observed mass = 11 600.4 ± 2.4 Da, calcd mass = 11 602 Da). d) HPLC-MS analysis of purified conjugate **12** (observed mass = 11 833.1 ± 2.1 Da, calcd mass = 11 835 Da).

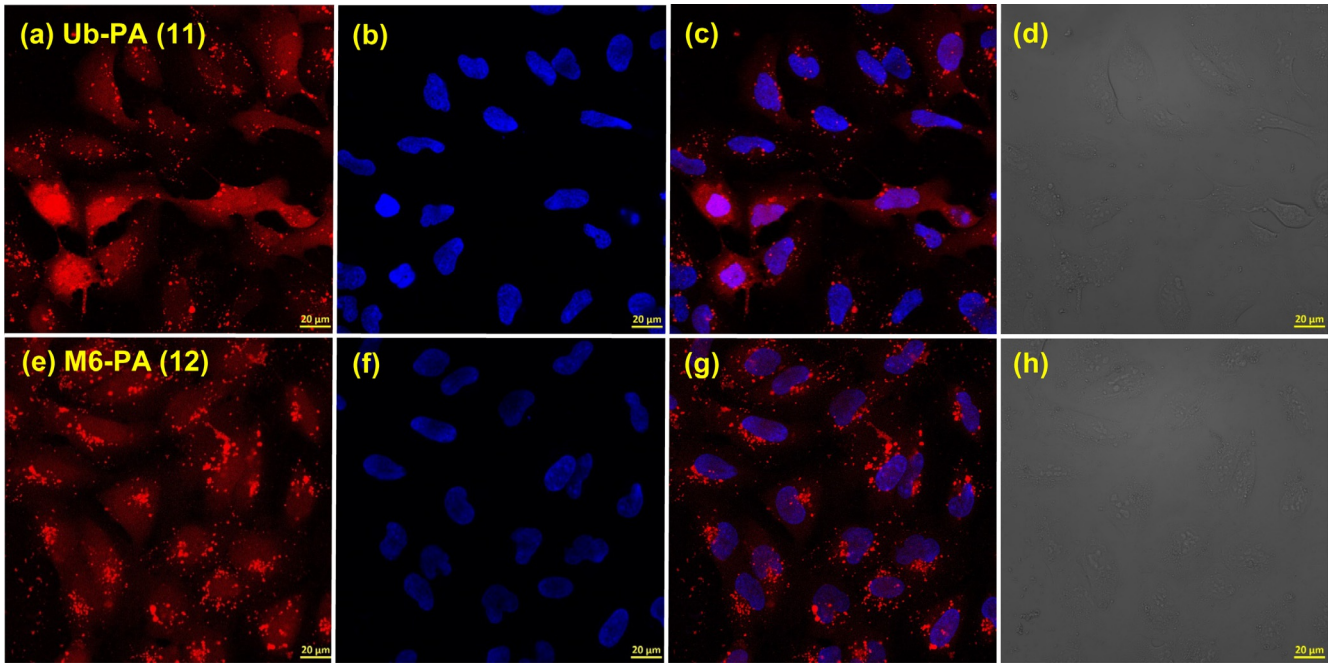

Figure 9. Representative images of delivery of **11** and **12** to live U2OS cells. a,e) TAMRA signal (red) from **11** and **12**, respectively. b,f) Hoechst (blue) from **11** and **12**, respectively. c) **11** (TAMRA) and Hoechst channel from (a) and (b) combined. g) **12** (TAMRA) and Hoechst channels from (e) and (f) combined. d,h) Bright field from **11** and **12**, respectively. (Scale bars 20 µm). The experiment was repeated thrice (imaging of at least 150 cells per experiment for each construct).

explore CPP mediated live-cell delivery of SUMO for further functional analysis.[22–25] SUMO plays important roles in many biological processes such as cell cycle progression, mitochondrial dynamics, and, genome stability by DNA repairing etc.[22,45,46] Although the name suggests ubiquitin-like, SUMO has only around 20% sequence identity with Ub and it is significantly larger (≈11 kDa) than Ub (≈8 kDa). SUMO exists in four different isoforms, SUMO-1, -2, -3, -4 and like

other post-translational modifications, SUMOylation can also be reversible by specific SUMO proteases, having potential as pharmacological targets.[47]

We designed fluorescently labelled SUMO2-**cR10** (**14**) and SUMO2-**cR10D** (**15**) analogues to verify the live-cell delivery efficiency upon DABCYL modification by visualizing their distribution in cell delivery by confocal microscopy and quantifying by a nuclear masking algorithm as stated earlier. The synthesis of the 93 amino acid long SUMO2 was carried out directly on solid support employing Fmoc-SPPS, having a solvent-exposed Cys48 to incorporate CPP moieties through disulfide linkage on the 2-CTC resin.[24] Upon coupling TAMRA to the N-terminus of SUMO2, the protein was cleaved from the solid support to give TAMRA-SUMO2 (**13**) in ≈6% isolated yield (Figure S25). Next, analogue **13** was conjugated to the activated **cR10** and **cR10D** peptides affording constructs **14** and **15**, respectively (Figure 10b,c).

After synthesizing analogues **14** and **15**, we examined the efficiency of the CPPs in live-cell delivery. We treated U2OS cells with 4 μM of **14** and **15**, dissolved in PBS and co-incubated at 37 °C for 45 min. Cells were then washed with heparin sulfate, followed by staining with Hoechst (nuclear stain). The CLSM images confirmed that analogue **15** was efficiently delivered and uniformly distributed in the cytoplasm and nucleus with significantly fewer signals in the lysosomes or endosomes (punctuates) as compared to analogue **14**, where there was considerably less fluorescence signal (Figure 11a,e; i,k).

To quantify the uptake efficiencies of SUMO2, we used a nuclear masking strategy following nuclear TAMRA intensity. The quantification of the total nuclear TAMRA intensity of the treated U2OS cells demonstrated a threefold increase in fluorescence intensity for **cR10D** compared to **cR10** (Figure 11m).

Conclusion

In this study, we have demonstrated that different fluorescently labelled synthetic proteins including Ub, Ub/Ubv based ABP and SUMO-2 analogues can be engineered to become cell-permeant by incorporating a new DABCYL-CPP. The DABCYL-CPP was incorporated either at N-terminus or on the solvent-exposed region of the protein scaffold bound through a cleavable disulfide linkage. With this developed CPP, our synthetic proteins in low micromolar concentrations can be efficiently delivered into live cells with the uniform cytosolic distribution. This CPP allowed us to substantially improve the concentration profile required for successful delivery, which is often a limitation for CPP mediated protein uptake. By comparing the DABCYL modified **cR10** (**cR10D**) with unmodified **cR10**, we were able to demonstrate the significance of single DABCYL modification resulting in a threefold increase in the cellular uptake of our synthetic Ub constructs, as confirmed by both qualitative and statistical analysis. Alongside, we investigated the importance of this modification on linear CPP, which showed comparable uptake efficiency of Ub analogue to the cyclic CPP. We used **cR10D** as a tool to assist the delivery of fluorescently labelled Ub-PA, an ABP for profiling different enzymes involved in the ubiquitination pathway and the USP7 selective Ubv based ABP. Our delivered ABPs allowed us to visualize ubiquitination machinery enzymes including USP7 through covalent labelling in live cells, which similarly can be used to advance our understanding of various DUBs by using the specific Ubvs.[43] We confirmed the applicability of **cR10D**, by delivering also fluorescently labelled SUMO-2-CPP analogues which opens up new opportunities to use cell-permeable SUMO ABPs for various applications and encourages the possibility of delivering a wide range of synthetic proteins for functional studies in live cells. We hypothesize that the DABCYL effect is due to its hydrophobic nature, although other effects might be important and yet to be determined.[10] We aim to further optimize the chemical space of the DABCYL structure for additional improvements of synthetic proteins delivery for functional studies in physiological environments. Intracellular delivery of functional synthetic proteins is a promising tool for understanding protein functions in general and therapeutic applications.

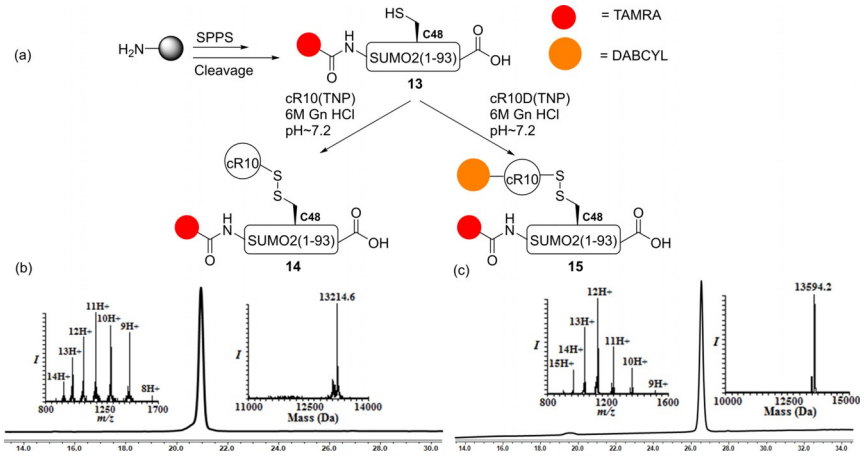

Figure 10. Synthesis of SUMO2-CPP conjugates: a) Synthetic scheme of **14** and **15** starting from **13**. b) HPLC-MS analysis of purified conjugate **14** (observed mass = 13214.6 ± 0.6 Da, calcd mass = 13214 Da). c) HPLC-MS analysis of purified conjugate **15** (observed mass = 13594.2 ± 0.2 Da, calcd mass = 13594 Da).

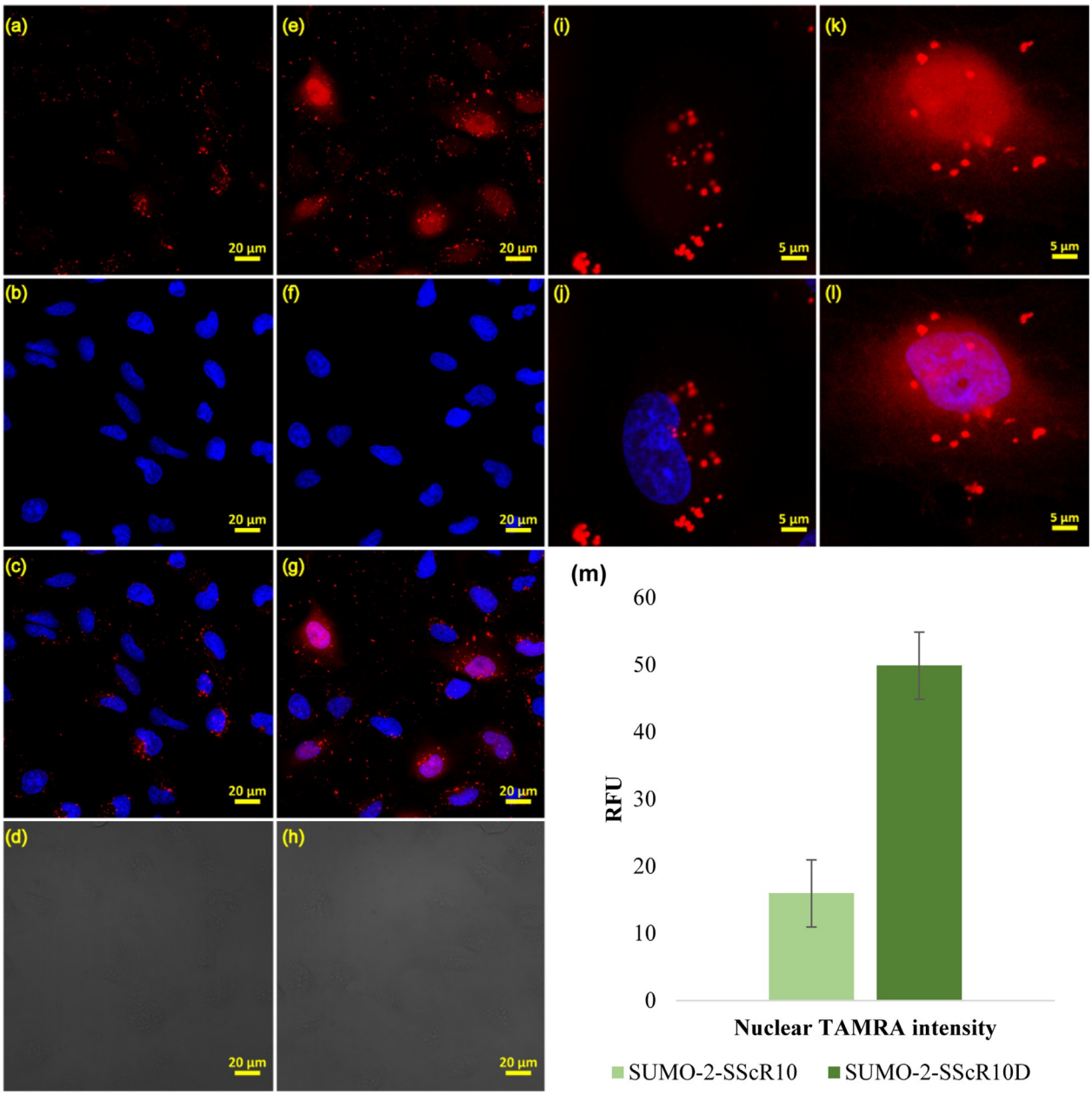

Figure 11. Representative images of delivery of **14** and **15** to live U2OS cells. a,e) TAMRA signal (red) from **14** and **15**, respectively. b,f) Hoechst (blue) from **14** and **15**, respectively. c) **14** (TAMRA) and Hoechst channel from (a) and (b) combined. g) **15** (TAMRA) and Hoechst channels from (e) and (f) combined. d,h) Bright field from **14** and **15**, respectively. (Scale bars 20 µm). The experiment was repeated thrice (imaging of at least 150 cells per experiment for each construct). i) Representative zoomed image of **14** from TAMRA channel and j) TAMRA and Hoechst channels combined. k) Representative zoomed image of **15** from TAMRA channel and l) TAMRA and Hoechst channels combined. (Scale bars 5 µm). m) Quantification of nuclear TAMRA intensity of **14** and **15** relative to the untreated cells. The result is the average of the three independent sets of experiments. Error bars are the standard deviation of averages.

Acknowledgements

A.B. holds The Jordan and Irene Tark Academic Chair. This project has received funding from the European Research Council (ERC) under the European Union's Horizon 2020 research and innovation program (grant agreement no. [831783]). G.M. is supported by the Gutwirth fellowship.

Conflict of interest

The authors declare no conflict of interest.

Keywords: activity-based probes · cell-penetrating peptides · fluorescence · small ubiquitin like modifier (SUMO) · ubiquitin

[1] A. Fu, R. Tang, J. Hardie, M. E. Farkas, V. M. Rotello, *Bioconjugate Chem.* **2014**, *25*, 1602 – 1608.

[2] K. Deprey, L. Becker, J. Kritzer, A. Plückthun, *Bioconjugate Chem.* **2019**, *30*, 1006 – 1027.
[3] A. T. Jones, E. J. Sayers, *J. Controlled Release* **2012**, *161*, 582 – 591.
[4] F. Duchardt, M. Fotin-Mleczek, H. Schwarz, R. Fischer, R. Brock, *Traffic* **2007**, *8*, 848 – 866.
[5] R. Brock, *Bioconjugate Chem.* **2014**, *25*, 863 – 868.
[6] G. Lättig-Tünnemann, M. Prinz, D. Hoffmann, J. Behlke, C. Palm-Apergi, I. Morano, H. D. Herce, M. C. Cardoso, *Nat. Commun.* **2011**, *2*, 453.
[7] P. G. Dougherty, A. Sahni, D. Pei, *Chem. Rev.* **2019**, *119*, 10241 – 10287.
[8] N. Nischan, H. D. Herce, F. Natale, N. Bohlke, N. Budisa, M. C. Cardoso, C. P. Hackenberger, *Angew. Chem. Int. Ed.* **2015**, *54*, 1950 – 1953; *Angew. Chem.* **2015**, *127*, 1972 – 1976.
[9] K. Najjar, A. Erazo-Oliveras, D. J. Brock, T. Y. Wang, J. P. Pellois, *J. Biol. Chem.* **2017**, *292*, 847 – 861.
[10] P. Zhang, L. L. Lock, A. G. Cheetham, H. Cui, *Mol. Pharm.* **2014**, *11*, 964 – 973.
[11] A. Ciechanover, *Best Pract. Res. Clin. Haematol.* **2017**, *30*, 341 – 355.
[12] A. F. L. Schneider, A. L. D. Wallabregue, L. Franz, C. P. R. Hackenberger, *Bioconjugate Chem.* **2019**, *30*, 400 – 404.
[13] M. P. C. Mulder, K. Witting, I. Berlin, J. N. Pruneda, K. P. Wu, J. G. Chang, R. Merkx, J. Bialas, M. Groettrup, A. C. O. Vertegaal, B. A. Schulman, D. Komander, J. Neefjes, F. El Oualid, H. Ovaa, *Nat. Chem. Biol.* **2016**, *12*, 523 – 530.
[14] D. S. Hameed, A. Sapmaz, L. Gjonaj, R. Merkx, H. Ovaa, *ChemBioChem* **2018**, *19*, 2553 – 2557.
[15] G. Mann, G. Satish, R. Meledin, G. B. Vamisetti, A. Brik, *Angew. Chem. Int. Ed.* **2019**, *58*, 13540 – 13549; *Angew. Chem.* **2019**, *131*, 13674 – 13683.
[16] W. Gui, C. A. Ott, k. Yang, J. S. Chung, S. Shen, S. Z. Zhuang, *J. Am. Chem. Soc.* **2018**, *140*, 12424 – 12433.
[17] A. E. Rabideau, B. L. Pentelute, *ACS Cent. Sci.* **2015**, *1*, 423 – 430.
[18] M. P. C. Mulder, K. F. Witting, H. Ovaa, *Curr. Issues Mol. Biol.* **2020**, *37*, 1 – 20.
[19] C. E. Weller, M. E. Pilkerton, C. Chatterjee, *Biopolymers* **2014**, *101*, 144 – 155.
[20] S. M. Mali, S. K. Singh, E. Eid, A. Brik, *J. Am. Chem. Soc.* **2017**, *139*, 4971 – 4986.
[21] P. Gopinath, S. Ohayon, M. Nawatha, A. Brik, *Chem. Soc. Rev.* **2016**, *45*, 4171 – 4198.
[22] S. Bondalapati, E. Eid, S. M. Mali, C. Wolberger, A. Brik, *Chem. Sci.* **2017**, *8*, 4027 – 4034.
[23] T. G. Wucherpfennig, V. R. Pattabiraman, F. R. Limberg, J. Ruiz-Rodríguez, J. W. Bode, *Angew. Chem. Int. Ed.* **2014**, *53*, 12248 – 12252; *Angew. Chem.* **2014**, *126*, 12445 – 12449.
[24] M. P. C. Mulder, R. Merkx, K. F. Witting, D. S. Hameed, D. El Atmioui, L. Lelieveld, F. Liebelt, J. Neefjes, I. Berlin, A. C. O. Vertegaal, H. Ovaa, *Angew. Chem. Int. Ed.* **2018**, *57*, 8958 – 8962; *Angew. Chem.* **2018**, *130*, 9096 – 9100.
[25] J. Bouchenna, M. Sénéchal, H. Drobecq, J. Vicogne, O. Melnyk, *Bioconjugate Chem.* **2019**, *30*, 2967 – 2973.
[26] R. Ekkebus, S. I. Van Kasteren, Y. Kulathu, A. Scholten, I. Berlin, P. P. Geurink, A. De Jong, S. Goerdayal, J. Neefjes, A. J. R. Heck, D. Komander, H. Ovaa, *J. Am. Chem. Soc.* **2013**, *135*, 2867 – 2870.
[27] S. Sommer, N. D. Weikart, U. Linne, H. D. Mootz, *Bioorg. Med. Chem.* **2013**, *21*, 2511 – 2517.
[28] H. D. Herce, D. Schumacher, A. F. L. Schneider, A. K. Ludwig, F. A. Mann, M. Fillies, M. A. Kasper, S. Reinke, E. Krause, H. Leonhardt, et al., *Nat. Chem.* **2017**, *9*, 762 – 771.
[29] A. Ciechanover, *Cell* **1994**, *79*, 13 – 21.
[30] F. E. Reyes-Turcu, K. D. Wilkinson, *Chem. Rev.* **2009**, *109*, 1495 – 1508.
[31] D. Komander, M. J. Clague, S. Urbé, *Nat. Rev. Mol. Cell Biol.* **2009**, *10*, 550 – 563.
[32] G. B. Vamisetti, R. Meledin, P. Gopinath, A. Brik, *ChemBioChem* **2019**, *20*, 282 – 286.
[33] G. Gavory, C. R. O'Dowd, M. D. Helm, J. Flasz, E. Arkoudis, A. Dossang, et al., *Nat. Chem. Biol.* **2018**, *14*, 118 – 125.
[34] T. Makio, R. W. Wozniak, *J. Cell Sci.* **2020**, https://doi.org/10.1242/jcs.237156.
[35] J. Borlido, V. Zecchini, I. G. Mills, *Traffic* **2009**, *10*, 1209 – 1220.
[36] M. Mäe, H. Myrberg, Y. Jiang, H. Paves, A. Valkna, U. Langel, *Biochim. Biophys. Acta Biomembr.* **2005**, *1669*, 101 – 107.
[37] H. Yukawa, H. Noguchi, I. Nakase, Y. Miyamoto, K. Oishi, N. Hamajima, et al., *Cell Transplant.* **2010**, *19*, 901 – 909.
[38] Y. W. Lee, D. C. Luther, R. Goswami, T. Jeon, V. Clark, J. Elia, et al., *J. Am. Chem. Soc.* **2020**, *142*, 4349 – 4355.
[39] R. Rezgui, K. Blumer, G. Yeoh-Tan, A. J. Trexler, M. Magzoub, *Biochim. Biophys. Acta Biomembr.* **2016**, *1858*, 1499 – 1506.
[40] G. Veggiani, M. C. R. Gerpe, S. S. Sidhu, W. Zhang, *Pharmacol. Ther.* **2019**, *199*, 139 – 154.
[41] S. M. Qi, G. Cheng, X. D. Cheng, Z. Xu, B. Xu, W. D. Zhang, J. J. Qin, *Front. Cell Dev. Biol.* **2020**, *8*, 1 – 14.
[42] A. Pozhidaeva, I. Bezsonova, *DNA Repair* **2019**, *76*, 30 – 39.
[43] A. Ernst, et al., *Science* **2013**, *339*, 590 – 595.
[44] L. Gjonaj, A. Sapmaz, R. González-Prieto, A. C. O. Vertegaal, D. Flierman, H. Ovaa, *Chem. Commun.* **2019**, *55*, 5075 – 5078.
[45] M. Nie, M. N. Boddy, *Biomolecules* **2016**, *6*, 14.
[46] S. P. Jackson, D. Durocher, *Mol. Cell* **2013**, *49*, 795 – 807.
[47] J. S. Seeler, A. Dejean, *Nat. Rev. Cancer* **2017**, *17*, 184 – 197.

Manuscript received: December 6, 2020
Version of record online: February 22, 2021

